

# QCD Tests in Hadronic Final States

M. Wobisch

III. Physikalisches Institut, RWTH Aachen  
D-52056 Aachen, Germany

## Abstract

Various QCD studies based on jet observables in hadronic final states in deep-inelastic scattering and hadron-hadron collisions are presented. Measured quantities are event shape variables, jet rates and jet cross sections. QCD analyses have been performed to determine the value of the strong coupling constant  $\alpha_s(M_Z)$ , the gluon density in the proton and to test power corrections.

Talk given on behalf of the H1 and the ZEUS Collaboration at the 29th International Conference on High-Energy Physics (ICHEP '98), Vancouver, Canada, July 23–29 1998.

# QCD TESTS IN HADRONIC FINAL STATES

M. WOBISCH

*III. Physikalisches Institut, RWTH Aachen, D-52056 Aachen, Germany,  
E-mail: Markus.Wobisch@desy.de*

Various QCD studies based on jet observables in hadronic final states in deep-inelastic scattering and in hadron-hadron collisions are presented. Measured quantities are event shape variables, jet rates and jet cross sections. QCD analyses have been performed to determine the value of the strong coupling constant  $\alpha_s(M_Z)$ , the gluon density in the proton and to test power corrections.

## 1 Introduction

Hadronic final states in high energy particle collisions offer a rich field for testing quantum chromodynamics (QCD). Especially suited for such studies are infrared and collinear safe “jet observables” for which QCD predictions can be calculated perturbatively. In this contribution measurements are presented of event shape variables<sup>1,2</sup>, jet rates<sup>3,4</sup> and jet cross sections<sup>5</sup> in deep-inelastic scattering (DIS) by the H1 and the ZEUS collaboration as well as jet cross sections in proton-antiproton collisions<sup>6</sup> by the CDF collaboration. These observables are directly (i.e. already at leading order) sensitive to the value of the strong coupling constant  $\alpha_s$ . Furthermore the jet cross sections are directly sensitive to the gluon density in the proton. For all these observables, the perturbative cross sections have been calculated to next-to-leading order (NLO) in  $\alpha_s$ . Based on these data, QCD analyses have been performed to extract the value of the strong coupling constant  $\alpha_s(M_Z)$  and to determine the gluon density in the proton. The event shape data have been analyzed for tests of “power corrections”.

## 2 Event Shape Variables in DIS

Event shape variables in deep-inelastic scattering events have been investigated over a large range of momentum transfers  $4 < Q < 100$  GeV, based on data taken at HERA by the H1 experiment<sup>1</sup> in 1994–1996 and by the ZEUS experiment<sup>2</sup> in 1995–1997. These event shapes are defined by linear sums of momenta of all hadronic final state particles in the current hemisphere of the Breit frame and are in different ways sensitive to the collimation of the energy flow along the event shape axis:

$$\text{Thrust: } T_z = \frac{\sum p_{\parallel}}{\sum |\vec{p}|} \quad (\tau_z = 1 - T_z),$$

$$T_c = \max_{\vec{n}_T} \frac{\sum |\vec{p} \cdot \vec{n}_T|}{\sum |\vec{p}|} \quad (\tau_c = 1 - T_c),$$

$$\text{Jet Broadness: } B_c = \frac{\sum p_{\perp}}{\sum |\vec{p}|},$$

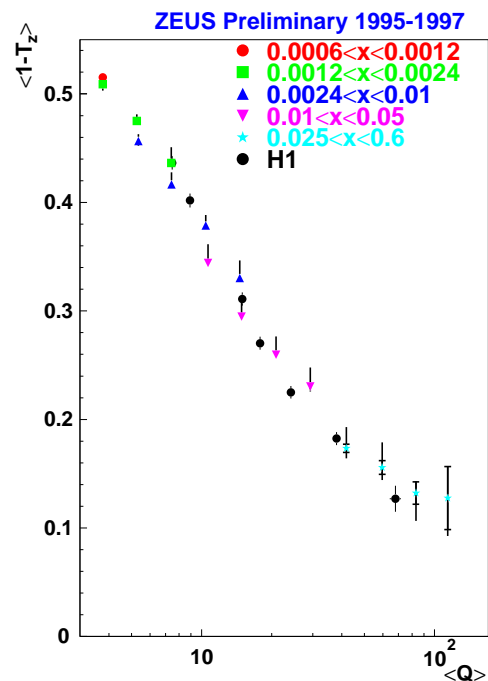


Figure 1: The  $Q$  dependence of the mean values of  $1 - T_z$  measured in deep-inelastic scattering in the current hemisphere of the Breit frame. The ZEUS data are measured in different bins of  $x_{Bj}$  while the H1 results are integrated over all  $x_{Bj}$ .

$$\text{Jet Mass: } \rho_E = \frac{(\sum p)^2}{2(\sum E)^2},$$

$$\rho_Q = \frac{(\sum p)^2}{Q^2}.$$

While in the analysis by the H1 collaboration only the dependence on the four-momentum transfer  $Q$  is measured (integrating over the Bjorken scaling variable  $x_{Bj}$ ), the ZEUS collaboration has also studied the dependence on  $x_{Bj}$ . The mean values of  $\tau_z$  are shown in Fig. 1 as a function of  $Q$ . The  $Q$  dependence of the mean values of the other event shapes is shown in Fig. 2. It can be seen that at larger values of  $Q$  and  $x_{Bj}$  the final state in the current hemisphere of the Breit frame is more collimated (relative to its total energy).

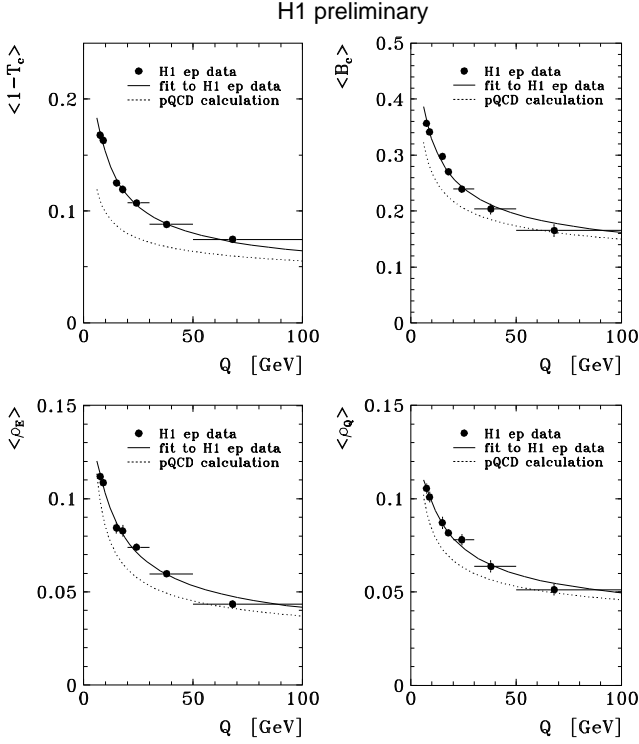


Figure 2: Event shape variables defined in the current hemisphere of the Breit frame in deep-inelastic scattering. Displayed is the  $Q$  dependence of the mean values of the different event shapes. The data are compared to the results of a QCD fit involving NLO predictions combined with power corrections. Also shown is the NLO prediction.

The QCD prediction for the mean value of any event shape  $\langle F \rangle$  can be written as a sum of perturbative and non-perturbative contributions:

$$\langle F \rangle = \langle F \rangle^{\text{pert}} + \langle F \rangle^{\text{pow}}, \quad (1)$$

with

$$\begin{aligned} \langle F \rangle^{\text{pert}} &= c_1 \alpha_s(Q) + c_2 \alpha_s^2(Q), \\ \langle F \rangle^{\text{pow}} &= a_F \frac{16}{3\pi} \frac{\mu_I}{Q} (\bar{\alpha}_0(\mu_I) - \alpha_s(Q) - b_0 \alpha_s^2(Q)). \end{aligned}$$

The perturbative part can be calculated to next-to-leading order. Apart from the dependence on the parton density functions (included in the coefficients  $c_i$ ) the only free parameter is  $\alpha_s$ . The non-perturbative contributions are modeled by  $a_F/Q$  power corrections, where the  $a_F$  have been calculated<sup>7</sup>. This contribution also depends on the value of  $\bar{\alpha}_0(\mu_I)$ , the effective coupling below the infrared matching scale  $\mu_I$ .

Fits have been performed to the mean values of the event shapes with the free parameters  $\alpha_s(M_Z)$  and  $\bar{\alpha}_0(\mu_I)$  according to eq. (1). The fit results in Fig. 2 show smaller non-perturbative contributions towards higher  $Q$ .

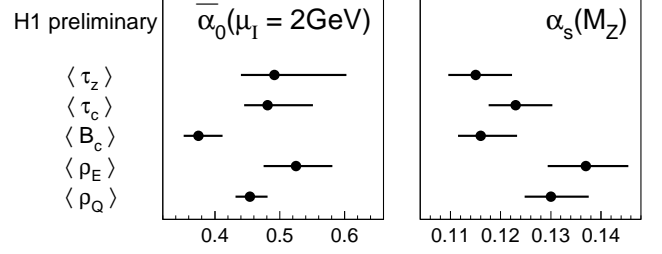


Figure 3: The results for  $\bar{\alpha}_0$  and  $\alpha_s$  as determined in a fit of the theoretical predictions based on NLO pQCD and power corrections to the  $Q$  dependence of the event shape mean values.

The resulting values of the strong coupling constant  $\alpha_s(M_Z)$  and  $\bar{\alpha}_0$  (displayed in Fig. 3) are of the same size and demonstrate approximately universal behavior for all event shapes. Remaining discrepancies may be traced back to large theoretical uncertainties: large NLO corrections and a large renormalization scale dependence indicate possible large contributions from higher, uncalculated orders.

### 3 Multijet Rates in DIS

To determine  $\alpha_s$ , the production rate of multijet events in DIS has been studied based on data taken in 1994 and 1995 by the H1 collaboration. Two analyses are presented where jets are defined by the modified JADE jet algorithm<sup>8</sup> (mJADE), applied in the HERA laboratory frame. In the mJADE jet definition the final state particles (and a pseudoparticle to account for the non-visible proton remnant) are clustered in the order of increasing invariant di-particle masses. For this jet definition the jet resolution parameter  $y_{ij}$  is given by  $y_{ij} = M_{ij}^2 / W^2$ , where  $W$  is the total invariant mass of the hadronic final state and  $M_{ij}$  is the smallest invariant mass between pairs of (pseudo-) particles.

Two observables have been measured: the  $y_2$  spectrum<sup>3</sup> and the (2+1)-jet rate<sup>4</sup>, the latter as a function of  $Q^2$ . The variable  $y_2$  is defined as the value of the jet resolution parameter  $y_{ij}$  at which exactly (2+1) jets are resolved (the “+1” denotes the proton remnant). The  $y_2$  spectrum has been measured for momentum transfers  $200 < Q^2 < 10000 \text{ GeV}^2$  (Fig. 4). The (2+1)-jet rate  $R_{2+1}$  is here defined as the fraction of DIS events that have (2+1) jets at a fixed value of the jet resolution parameter  $y_{\text{cut}} = 0.02$  (i.e. the rate of events which have (2+1) jets after the clustering has been stopped when all  $M_{ij}^2/W^2 > 0.02$ ). The results have been obtained in four  $Q^2$  bins at  $40 < Q^2 < 4000 \text{ GeV}^2$  (Fig. 5 top).

Both measurements have been used to extract  $\alpha_s(M_Z)$ . For the  $y_2$  spectrum, a fit has been performed to determine  $\alpha_s$  at a scale of  $\mu_r^2 = \langle Q^2 \rangle = 620 \text{ GeV}^2$ . Using



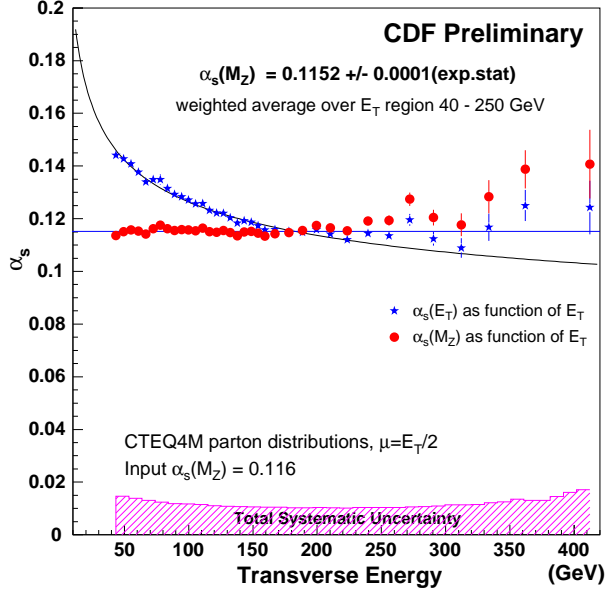


Figure 6: The values of the strong coupling constant  $\alpha_s(E_T/2)$  and  $\alpha_s(M_Z)$  as determined from the inclusive jet cross section in  $\bar{p}p$ -collisions. The single values have been evolved to  $\mu = M_Z$  using the two-loop formula. The error weighted average over the  $E_T$  range 40 – 250 GeV gives the final result of  $\alpha_s(M_Z) = 0.115$ .

Each of the 36 individual bins in  $E_T$  allows to extract a value of  $\alpha_s$  at a scale chosen to be  $\mu = E_T/2$ <sup>6</sup>. The single  $\alpha_s(E_T/2)$  values have been evolved to  $\alpha_s(M_Z)$  using the two-loop equation (Fig. 6). By forming an error weighted average over the  $E_T$  range 40 – 250 GeV, an average value of  $\alpha_s(M_Z)$  has been obtained (the exclusion of the points  $E_T > 250$  GeV avoids possible bias by the population of events at high  $E_T$ ). For the CTEQ4M parton distributions, the result is

$\alpha_s(M_Z) = 0.1152 \pm 0.0001(\text{stat.})^{+0.0083}_{-0.0093}(\text{exp.syst.})$  with a theoretical uncertainty of  $\pm 0.005$  from the renormalization scale dependence<sup>10</sup>.

The result also depends on the parton densities used in the NLO calculation. This dependence is demonstrated in Fig. 7 where the resulting  $\alpha_s(M_Z)$  value is shown as a function of the  $\alpha_s(M_Z)$  used in the global fit of the parton densities. A clear correlation is seen which reflects the dependence of the inclusive jet cross section on the gluon density  $g(x)$  in the proton. The size of the gluon density in different global fits is anti-correlated to the assumed value of  $\alpha_s$ , since most cross sections only depend on the product  $\alpha_s \cdot g(x)$ .

Due to the dependence of the extracted  $\alpha_s(M_Z)$  on the parton densities (and their  $\alpha_s$  value) this analysis can not be seen as an independent measurement. However, the fact that for standard parton distributions (as CTEQ4M) the extracted  $\alpha_s$  is close to the  $\alpha_s$  used in the parton densities is an important demonstration of consistency.

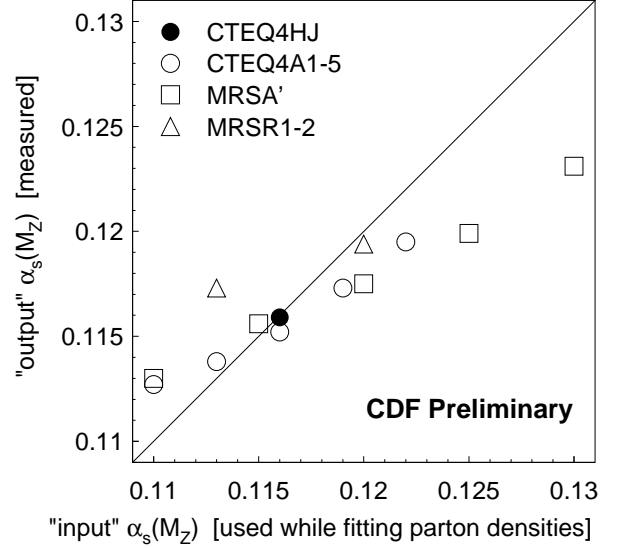


Figure 7: The values of the strong coupling constant  $\alpha_s(M_Z)$  as derived from a QCD fit to the inclusive jet cross section in  $\bar{p}p$ -collisions. Several fits have been performed for different parameterizations of parton density functions. Shown is the dependence of the central fit result of  $\alpha_s(M_Z)$  on the value of  $\alpha_s(M_Z)$  used in the fit of the parton distributions.

## 5 Dijet Cross Sections in DIS

To determine the gluon density in the proton, dijet production in deep-inelastic scattering has been studied by the H1 collaboration based on data taken in 1994–1997<sup>5</sup>. The dijet cross section has been measured for different  $k_\perp$ -type jet algorithms in the Breit frame. QCD models predict that hadronization corrections are smallest for the longitudinally boost-invariant  $k_\perp$  jet algorithm<sup>11</sup> (about 7% with negligible model dependence).

For this algorithm the inclusive dijet cross section has been measured as a function of several observables:  $Q^2$ ,  $x_{Bj}$ , the average transverse jet energy of the two jets in the Breit frame  $\bar{E}_T$ , the invariant dijet mass  $M_{jj}$  and the variable  $\xi = x_{Bj}(1 + M_{jj}^2/Q^2)$  which is (at leading order) equal to the momentum fraction of the proton carried by the parton that enters the hard process. Dijet events have been selected where at least two jets have transverse energies of  $E_T > 5$  GeV in the Breit frame. In addition, the sum of the transverse jet energies of the two highest  $E_T$  jets in the event has been required to be  $E_{T1} + E_{T2} > 17$  GeV.

The dijet cross section is shown in different bins of  $Q^2$  as a function of  $\bar{E}_T$  (Fig. 8) and the variable  $\xi$  (Fig. 9) for  $10 < Q^2 < 5000$  GeV<sup>2</sup>. The data are compared to the NLO prediction for different renormalization scales. Reasonable agreement is observed, except at smaller values of  $\xi$  where the NLO prediction is slightly too low.

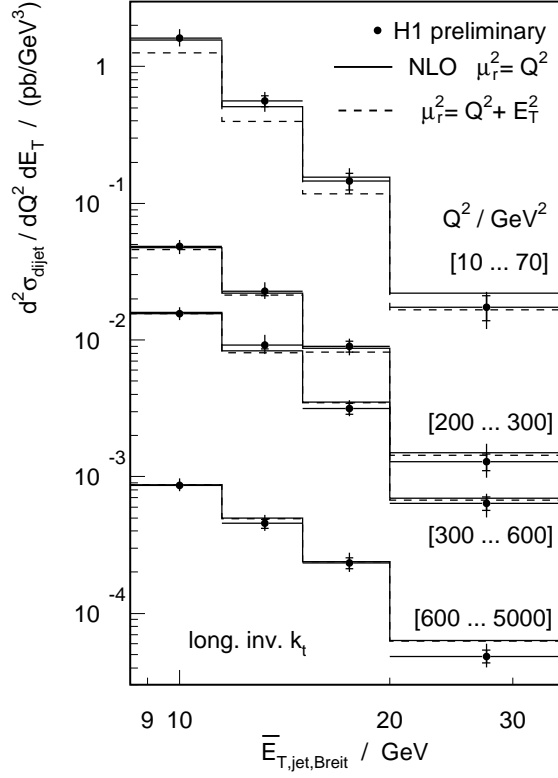


Figure 8: The double differential dijet cross sections  $d^2\sigma/dQ^2 d\bar{E}_T$  in deep-inelastic scattering. The data are compared to the NLO prediction for two different choices of the renormalization scale for CTEQ4M parton distributions.

The determination of the gluon density in a QCD fit to these dijet cross sections also requires knowledge of the quark densities and of  $\alpha_s$ . In the present analysis  $\alpha_s(M_Z)$  has been taken to be the world average<sup>12</sup> within its uncertainty ( $\alpha_s(M_Z) = 0.119 \pm 0.005$ ) and subsequently evolved to the relevant scales using the two-loop equation. To have a consistent treatment of the quark densities in the QCD fit, H1 data on the inclusive neutral current DIS cross section<sup>13</sup> at  $200 < Q^2 < 650 \text{ GeV}^2$  have been included in the fit. These data give strong constraints on the quark densities.

The NLO corrections to the dijet cross sections at  $Q^2 \lesssim 100 \text{ GeV}^2$  are sizeable (50 – 100 %) and the renormalization scale dependence is large (up to 20 %). To avoid these theoretical uncertainties, only dijet data at  $Q^2 > 200 \text{ GeV}^2$  have been considered in the fit. In this range, approx. 55 % of the dijet cross section is gluon induced. To maximize the sensitivity to the  $x$ -dependence of the gluon density, the fit has been performed on the double differential cross sections  $d^2\sigma/dQ^2 d\xi$  and  $d^2\sigma/dQ^2 dx_{Bj}$ . The gluon and quark densities have been fitted at a factorization scale of  $\mu_f^2 = 200 \text{ GeV}^2$  which is of the size of the hard scales for both the dijet and

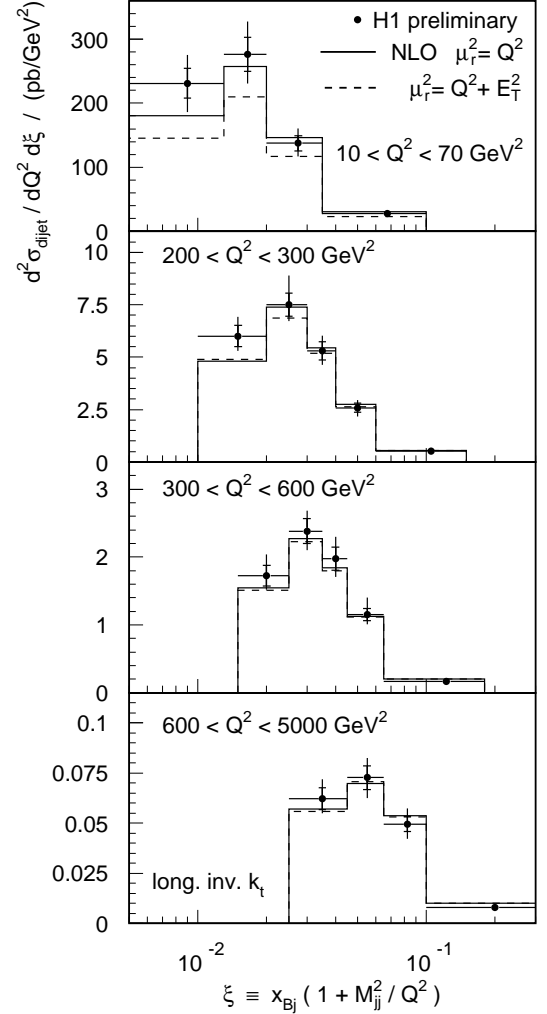


Figure 9: The double differential dijet cross sections  $d^2\sigma/dQ^2 d\xi$  in deep-inelastic scattering. The data are compared to the NLO prediction for two different choices of the renormalization scale for CTEQ4M parton distributions.

the inclusive cross section (dijet cross section:  $\mu_f^2 \simeq \bar{E}_T^2$ , inclusive cross section:  $\mu_f^2 \simeq Q^2$ ). The  $x$ -dependence of the gluon and quark densities has been parameterized by the usual 3-, 4- or 5-parameter functions<sup>5</sup>.

The gluon density obtained from the QCD fit with its error band is shown in Fig. 10 in the range  $0.01 < x < 0.1$ . This result extends the  $x$ -range from previous gluon determinations from H1 structure function data to larger  $x$ -values. The uncertainty is dominated by the error of  $\alpha_s$ , the renormalization scale dependence of the NLO calculation and the uncertainty in the absolute calorimetric energy scale. While the result is slightly higher than the results of different global analyses (although compatible within the error) it is in good agreement with the gluon density from a QCD analysis of H1 structure function data.

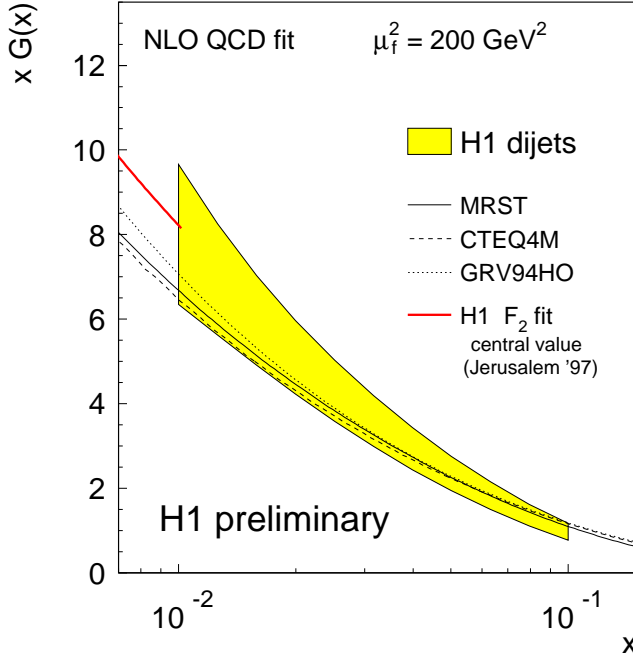


Figure 10: The gluon density in the proton in the  $\overline{MS}$ -scheme determined in a NLO QCD fit to dijet cross sections for a value of  $\alpha_s(M_Z) = 0.119 \pm 0.005$ . The error band is compared to the gluon densities obtained in global fits and to the result of a QCD fit to H1 structure function data (only the central value without error band).

## Summary

Measurements of jet observables in hadronic final states in deep-inelastic scattering and in hadron-hadron collisions have been presented. Based on perturbative QCD calculations in next-to-leading order, fits to the data have been performed to extract the value of the strong coupling constant  $\alpha_s(M_Z)$  and the gluon density in the proton. The results are consistent with each other and in agreement with world average values.

The precision of these results is limited by uncertainties in the perturbative predictions (renormalization scale dependence) and by the correlation between the gluon density and  $\alpha_s$ . Further progress will require combined analyses of different data sets for consistent, simultaneous determinations of  $\alpha_s$  and the gluon density.

The “power correction” approach gives a fair description of hadronization corrections to DIS event shape data. Further developments in this field will improve the understanding of non-perturbative physics and may allow to describe non-perturbative contributions to different processes in a universal way.

## References

1. H1 Collab., paper 530 of the 29th Intern. Conf. on High-Energy Physics, Vancouver, Canada (1998).
2. ZEUS Collab., paper 808 of the 29th Intern. Conf. on High-Energy Physics, Vancouver, Canada (1998).
3. H1 Collab., paper 528 of the 29th Intern. Conf. on High-Energy Physics, Vancouver, Canada (1998).
4. H1 Collab., paper 527 of the 29th Intern. Conf. on High-Energy Physics, Vancouver, Canada (1998).
5. H1 Collab., paper 520 of the 29th Intern. Conf. on High-Energy Physics, Vancouver, Canada (1998).
6. CDF Collaboration, (1998)  
[www-cdf.fnal.gov/physics/new/qcd/QCD.html](http://www-cdf.fnal.gov/physics/new/qcd/QCD.html).
7. M. Dasgupta, B.R. Webber, *Eur. Phys. J. C* 1 (1998) 539.
8. D. Graudenz and N. Magnussen, Proc. Workshop Physics at HERA, Hamburg, Vol. 1 (1991) 261.
9. V.D. Elvira, proc. of 33rd Rencontres de Moriond, Les Arcs, France (1998).
10. W. Giele et al., *Phys. Rev. D* 53 (1996) 120.
11. S.D. Ellis, D.E. Soper, *Phys. Rev. D* 48 (1993) 3160.
12. S. Catani, [hep-ph/9712442](http://hep-ph/9712442).
13. H1 Collab., paper 262 of the Intern. Europhysics Conf. on High-Energy Physics, Jerusalem, Israel (1997).